Electronic Supplementary Material (ESI) for Lab on a Chip.

Automated high-content phenotyping from the first larval stage till onset of adulthood of the nematode *Caenorhabditis elegans*

Supplementary Information

H. B. Atakan[1], M. Cornaglia[1], L. Mouchiroud[2], J. Auwerx[2] and M. A. M. Gijs[1]

[1]Laboratory of Microsystems, Ecole Polytechnique Fédérale de Lausanne, CH-1015 Lausanne, Switzerland

[2]Laboratory of Integrative Systems Physiology, Ecole Polytechnique Fédérale de Lausanne, CH-1015 Lausanne, Switzerland

Supplementary Figures

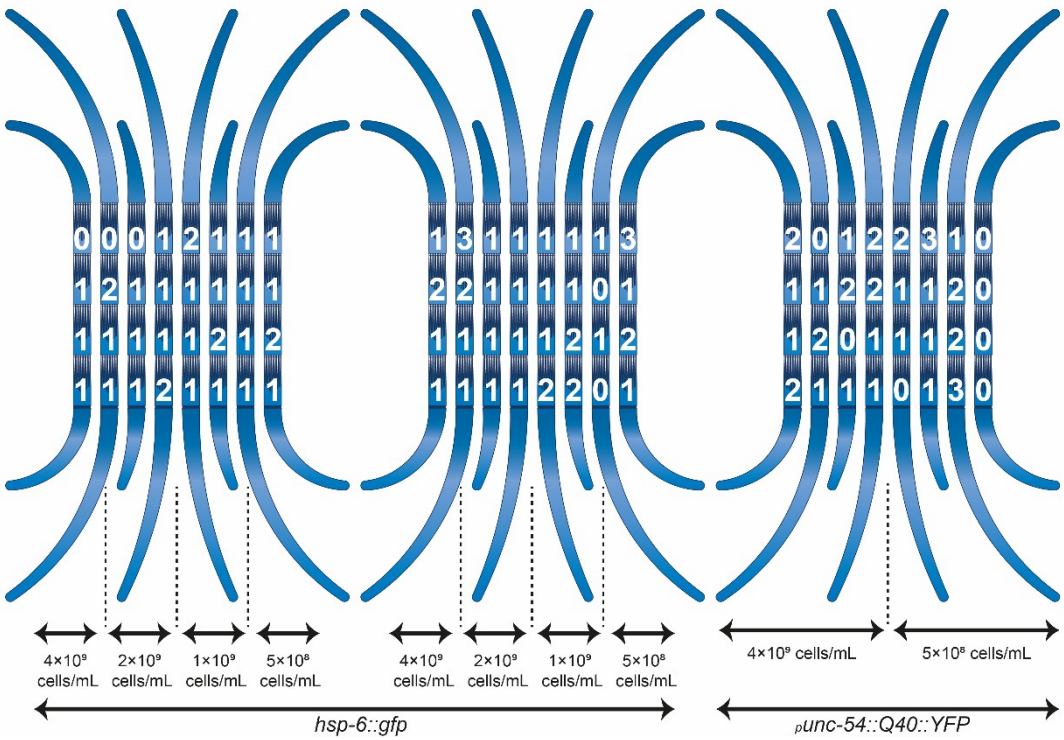

Fig. S1 Schematic representation of an experimental configuration, as defined by the number of worms distributed over the different chambers and the applied feeding conditions. For *hsp-6::gfp* nematode experiments, 4×10^9 cells/mL, 2×10^9 cells/mL, 1×10^9 cells/mL, and 5×10^8 cells/mL were required; therefore two lanes were selected per feeding condition. These experimental conditions were repeated on a second identical chip in order to obtain significance in worm phenotyping. For *$_p$unc-54::Q40::YFP* nematode experiments, 4×10^9 cells/mL and 5×10^8 cells/mL were required; therefore four lanes were used per feeding condition. A single chip was capable of significant worm phenotyping.

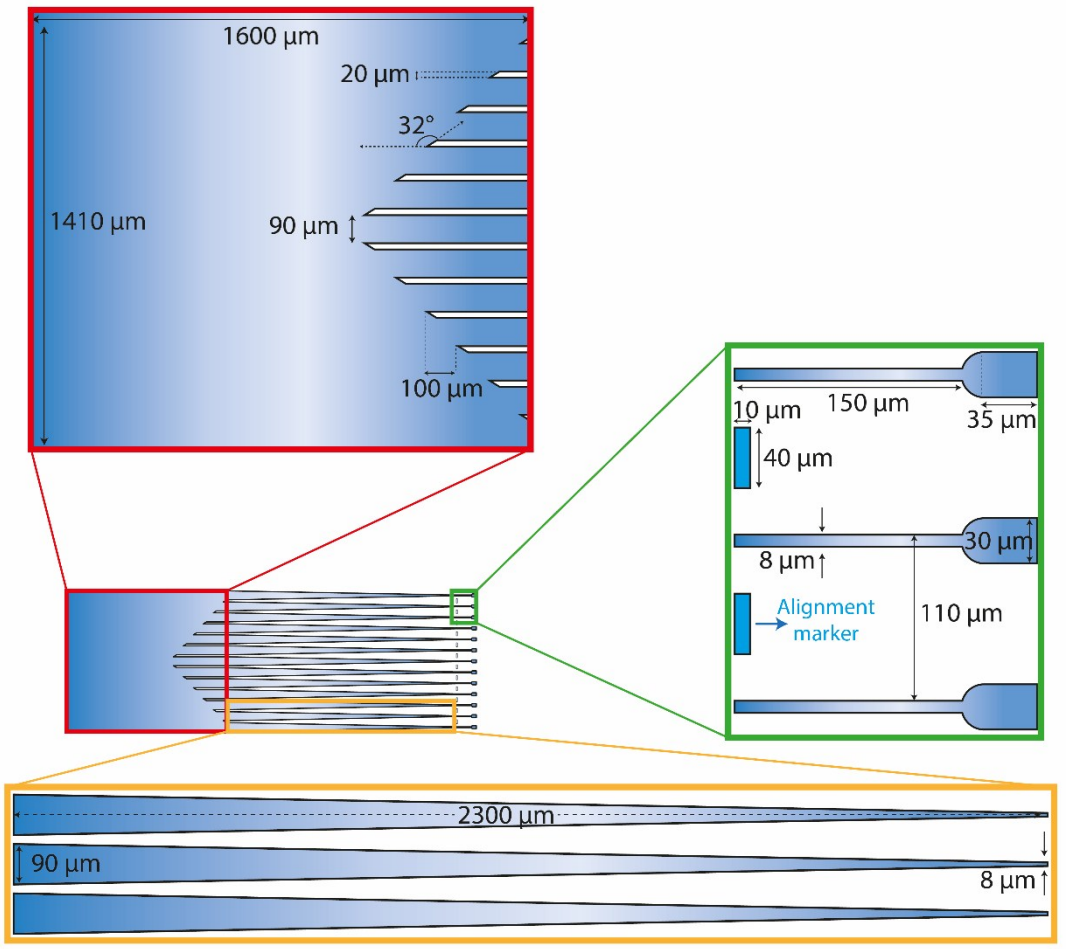

Fig. S2 The schematic representation of a unit cell (consisting of a growth chamber and thirteen tapered channels) with zoom on certain areas including the specific dimensions. Each tapered channel entrance has a width of 90 µm, which permits the adult worms to enter, and gradually drops down to 8 µm, preventing L1 worms to cross to the neighboring chamber. This 8 µm filter size is also critical for the passive hydrodynamic distribution of the worms among the chambers. The entrance of the tapered channel arrays has also been given a tapered shape with an angle of 32° to bend the worms towards the tapered channels effortlessly and to increase the success of the confinement. We carefully selected all the geometrical parameters so that we could have spacious growth chambers that can accommodate up to three worms, angled entrances of the tapered channels to provide good immobilization rates, large enough channel entrances to confine all the stages of worms, short enough tapered channel exit points to block the small larvae during confinement and to provide bacterial passage. We also included alignment markers to line up the camera position perfectly on the confinement channels.

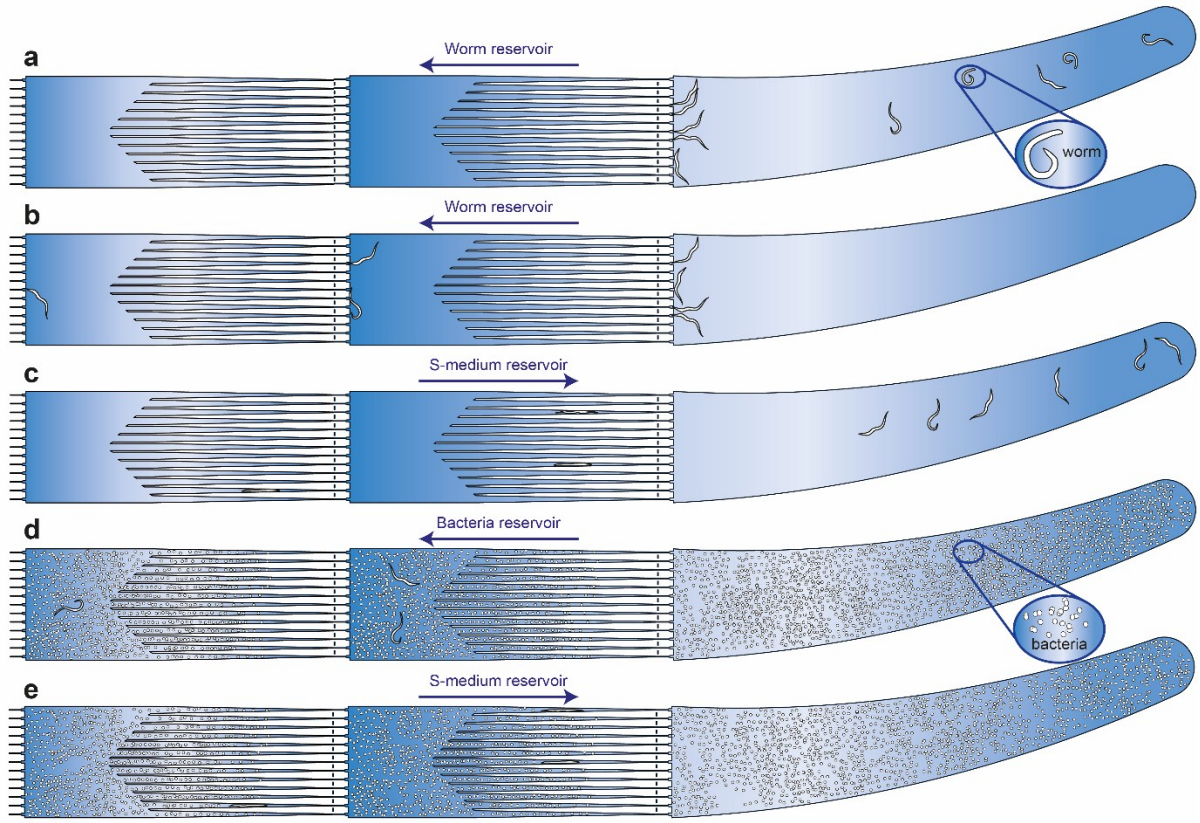

Fig. S3 Operation modes of the microfluidic chip. (a) A 200 µL suspension of synchronized L1 worms in S-medium is injected from the media outlet of a lane towards the media inlet (chip connections (iii) and (ii) in Fig. 1f). (b) After successfully collecting L1 worms in front of the first filter set, the worms are distributed over all unit cells by applying short injection pulses. (c) When the desired worm distribution among the growth chambers is reached, excessive worms are gently pushed back towards the media outlet (chip connections (i) and (iii) in Fig. 1f). (d) A 25 µL suspension of *E. coli* is injected from the media outlet until it completely fills the microfluidic chip (chip connections (iii)' and (ii) in Fig. 1f). (e) The automated imaging protocol starts with a first cycle of worm confinement in the tapered channels (chip connections (i) and (iii)' in Fig. 1f).

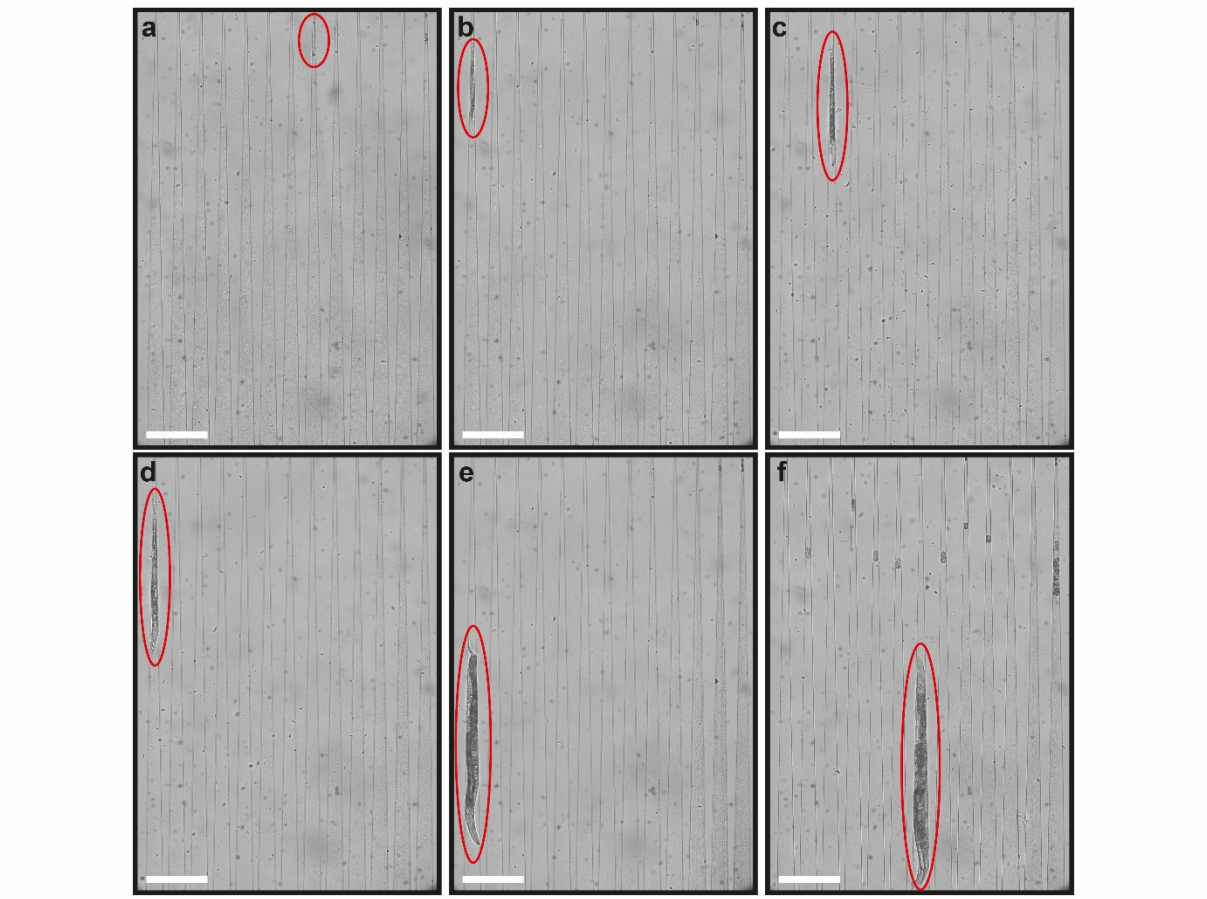

Fig. S4 Confinement images of (a) L1, (b) L2, (c) L3, (d) L4 larvae, (e) young adults, and (f) adults. Scale bars: 300 μm.

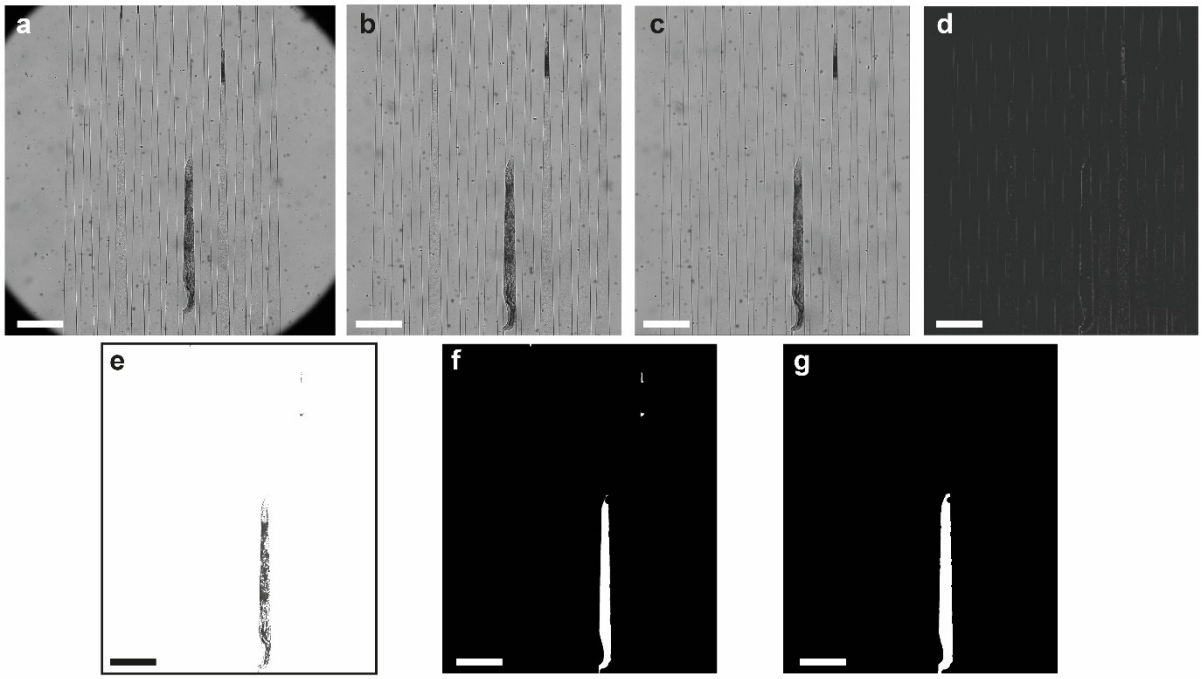

Fig. S5 Details of the automated image analysis for the worms confined in the tapered channels. (a) All worms in the growth chambers are confined and a 2048 by 2048 pixel image is acquired. (b) The image is cropped to reduce the data storage, leaving only thirteen channels in the field of view. (c) The image is slightly blurred to reduce the false detections. (d) A dynamic background is created for each individual image and subtracted from the slightly blurred image (see details in Fig. S9). (e) Image intensity values are adjusted such that background saturates towards white, the worms and outliers towards zero. (f) The image is thresholded. (g) The largest connected components matching to the number of worms accommodated in that chamber are detected. Scale bars: 300 μm.

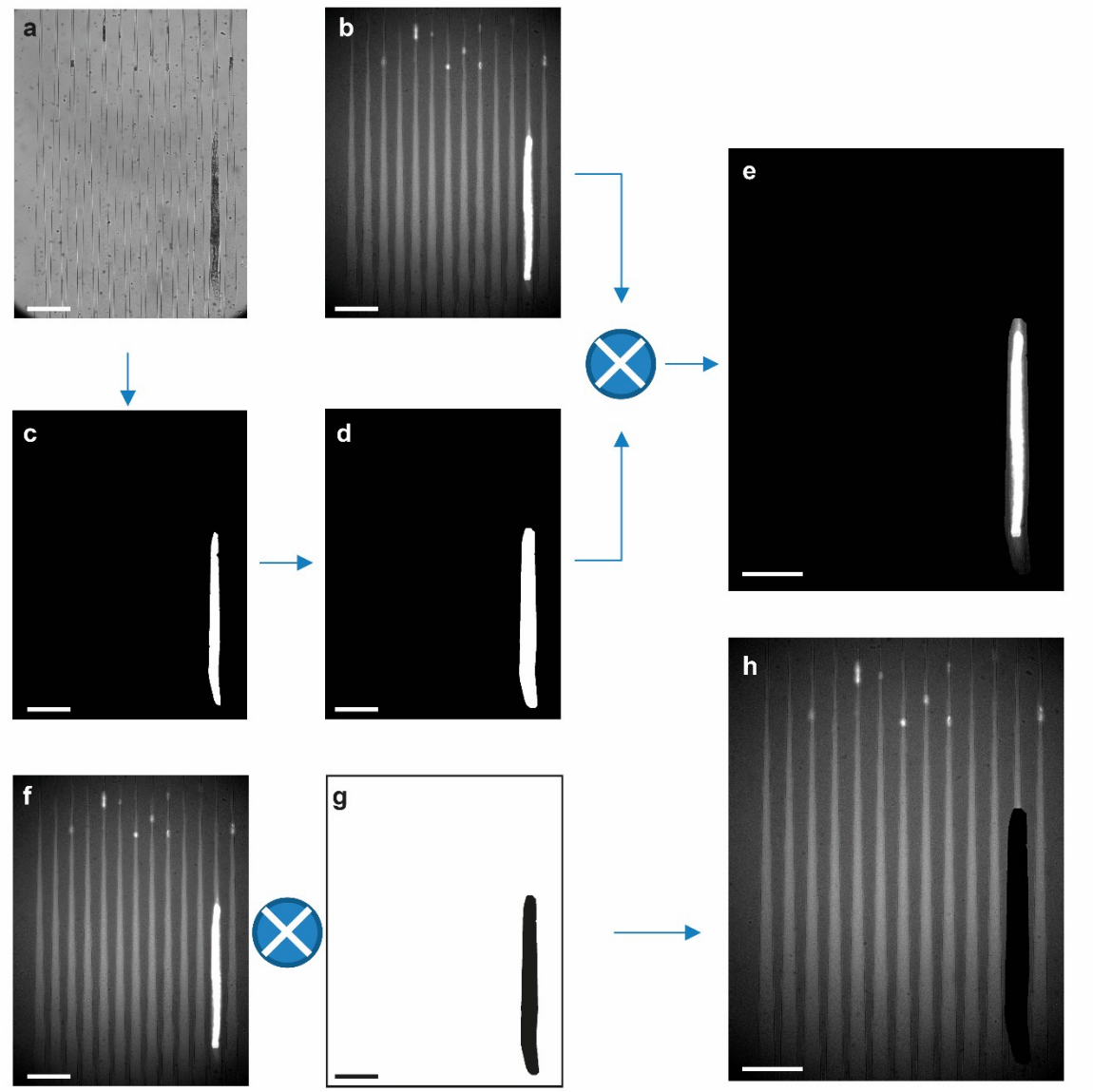

Fig. S6 Details of the automated fluorescent image intensity analysis for the worms confined in the channels. All worms in the growth chambers are confined and a brightfield image (a) and a fluorescent image (b) are acquired. (c) The brightfield image is turned into a binary mask as explained in Fig. S5. (d) This mask is dilated to ensure the full coverage of the worm during the multiplication with the fluorescent image in (b). (e) The resultant image is used to quantify the fluorescent signal expression only inside the worms. (f) The same fluorescent image is also processed to quantify the background intensity. (g) The inverted version of binary mask in (d) is used to exclude all the worms in the image. (h) These two images are multiplied to obtain a worm-free background fluorescent image to quantify the average background fluorescent intensity expression. The average fluorescent intensity value was calculated by taking the median of all non-zero intensity values inside each identified worm mask. Likewise, the average of all non-zero intensity values were calculated and scored as the average background intensity for the second part. Scale bars: 300 μm.

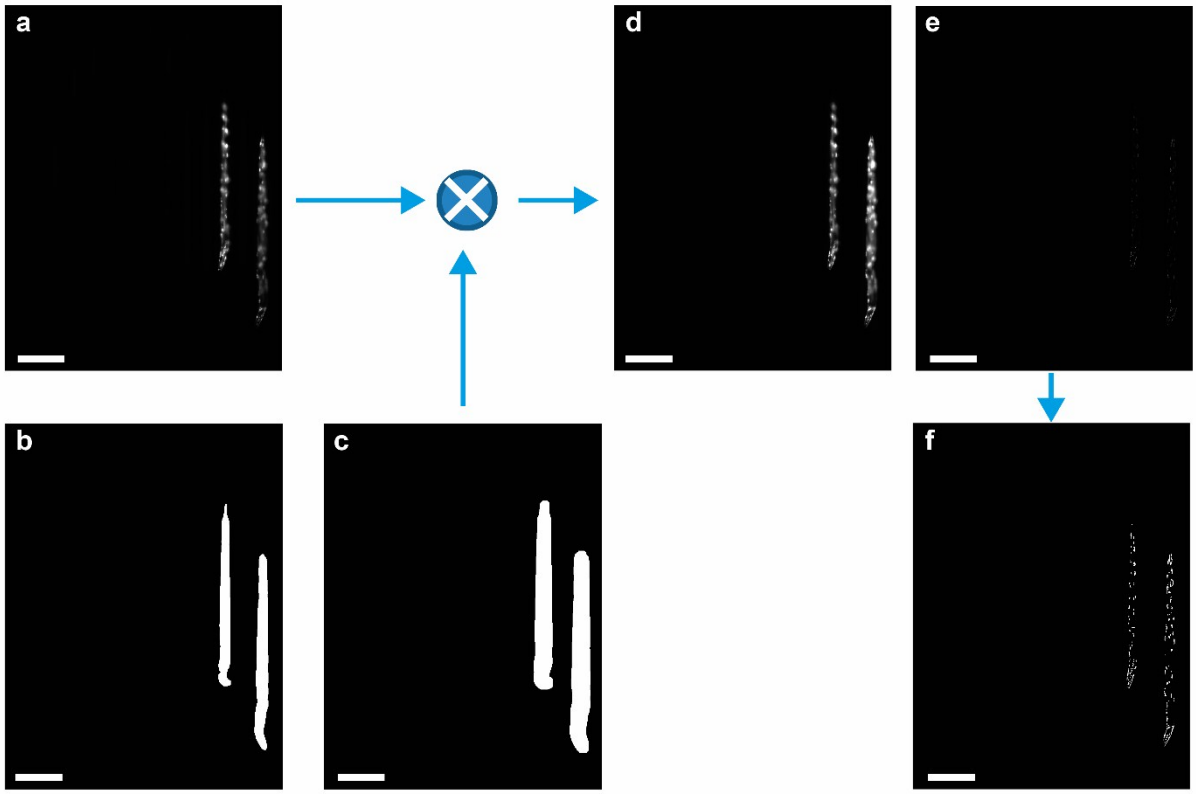

Fig. S7 Details of the automated fluorescent image aggregate analysis for the *$_p$unc-54::Q40::YFP* worms confined in the channels. (a) A fluorescent image is captured while the worms are confined in tapered channels. (b) The resultant image from the brightfield confinement analysis is loaded, (c) and dilated so that it covers the worms of interest after the image multiplication. (d) The resultant multiplied image is background-free and contains only the worms. (e) The image is passed through a Laplacian of Gaussian filter (σ=10) to detect the aggregates. (f) It is, then, thresholded to observe the aggregates clearly. A connected component search was performed to count the number of aggregates and record the total aggregate area by counting the total number of non-zero pixels. As the worms were confined in the tapered channels, some clusters that were in different focal planes were not easily detected; however, the resultant image provided accurate results to observe the significant aggregates. Scale bars: 300 μm.

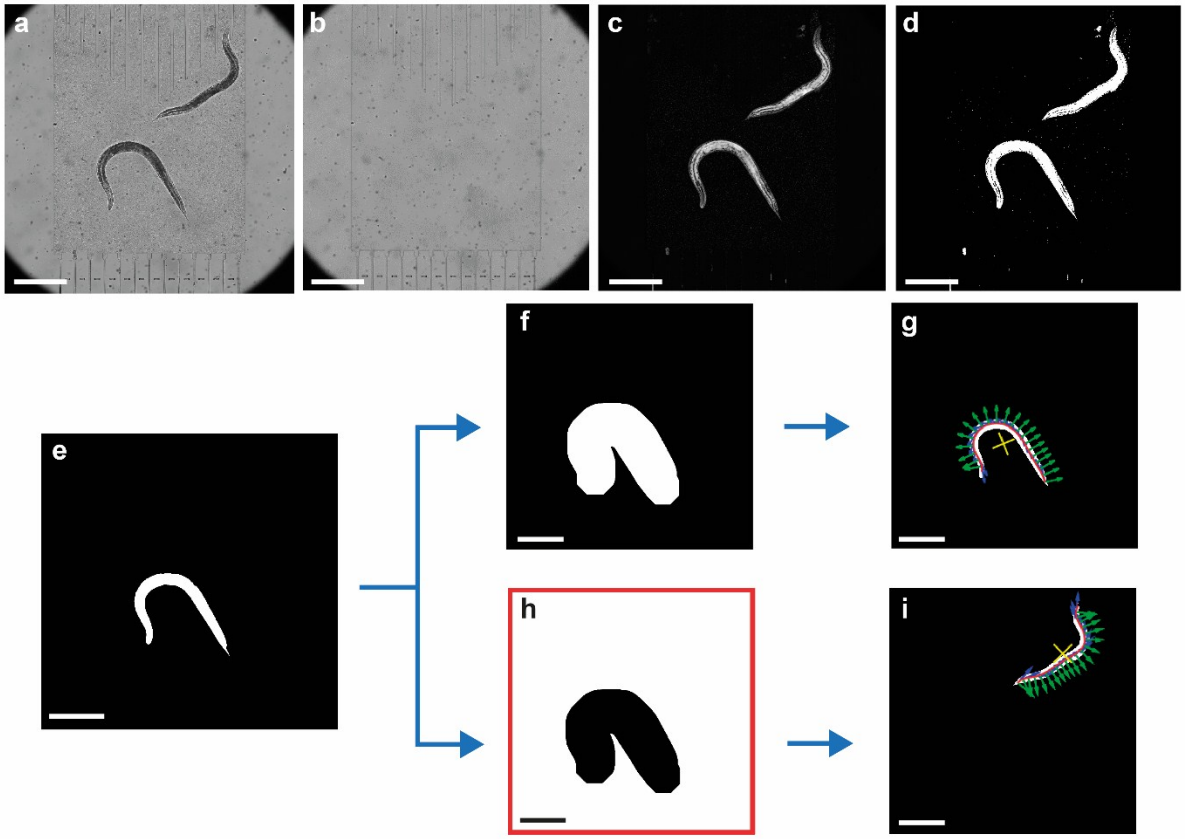

Fig. S8 Details of the automated motility analysis for worms that are freely moving in a growth chamber. (a) Video frames at 5 Hz for 10 seconds are recorded. (b) A dynamic background is created for each video set as explained in Fig. S9. (c) All the video frames are removed from their background. (d) The subtracted image is thresholded and smoothed. (e) One of the largest connected components is detected. Hereon, our algorithm was divided into two parts. In the first part, the first detected worm's mask was dilated (f) and multiplied with the binarized version of the consecutive frame to keep track of the same worm. A spline is fit, tangential and perpendicular components of the spline are marked for further data extraction (g). Among the two end points of the spline, the higher curvature point was assumed to be the head and the other end to be the tail. In the second part, we wanted to detect other neighboring worms in the same growth chamber. An inverted version of mask in (f) is multiplied with the first frame of the same video set (d) in order to keep track of the other worms in the chambers (h). The same approach as in (g) is pursued to obtain all the necessary components for data extraction (i). If there were more than two worms in the same growth chamber, we combined the dilated and inverted versions of the first tracked frame with a logical OR. Scale bars: 400 µm.

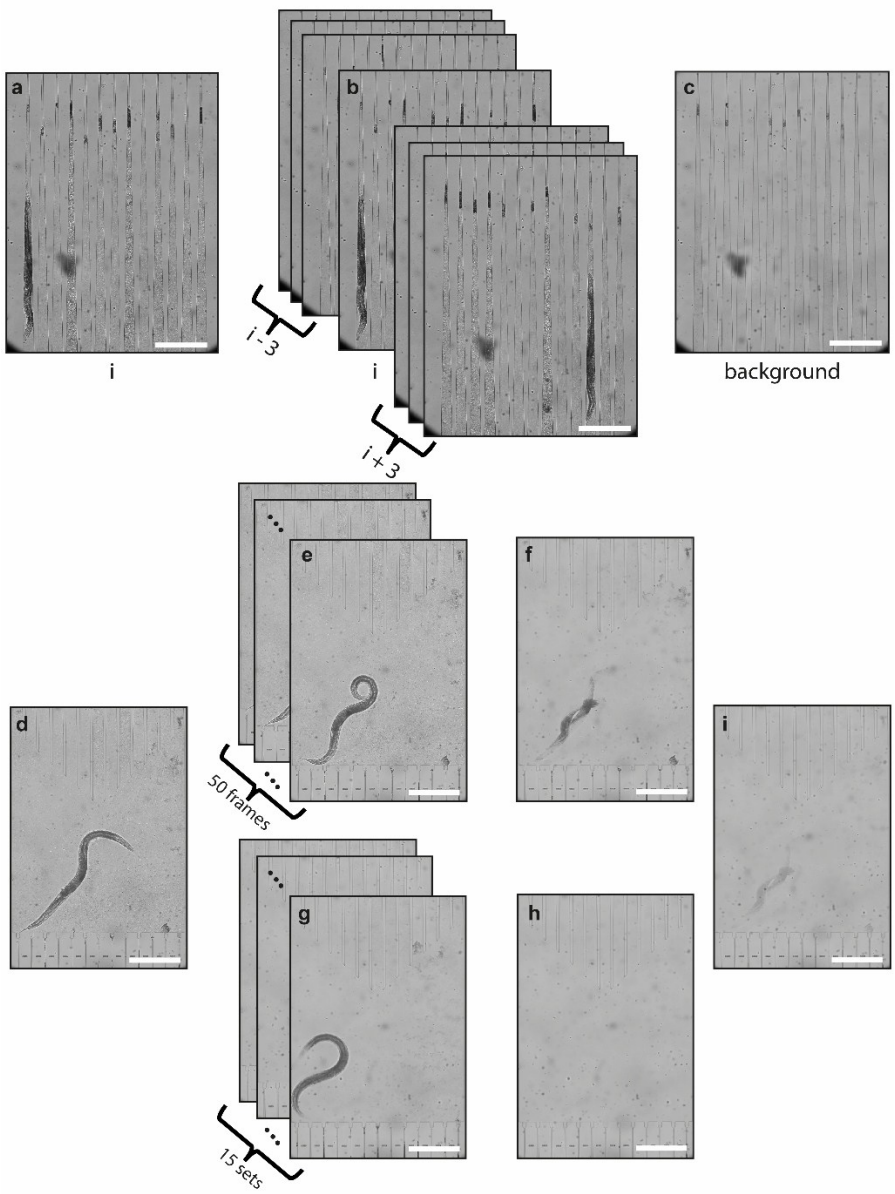

Fig. S9 The dynamic background creation approach used in the confinement and motility analysis. (a) An image is acquired during the confinement cycle when all the worms in the chambers are immobilized in tapered channels. (b) The image of interest, the previous three frames and the following three frames are merged by taking the median. (c) The resultant median filtered image is worm-free and takes into account the bacteria clusters in the tapered channels for a more accurate worm shape extraction. (d) An image is acquired during the worm motion in the growth chamber. (e) The images of each video set, having 50 frames typically, are merged together to obtain the "video set" background (f). (g) The 15 sets of "video set" background are merged together to obtain the "overall" background (h). (i) For each video set, two units of "video set" background and one unit of "overall" background are averaged to obtain one "final" background, which results in the best distinction of the worms in the chambers from the environment. Scale bars: 400 μm.

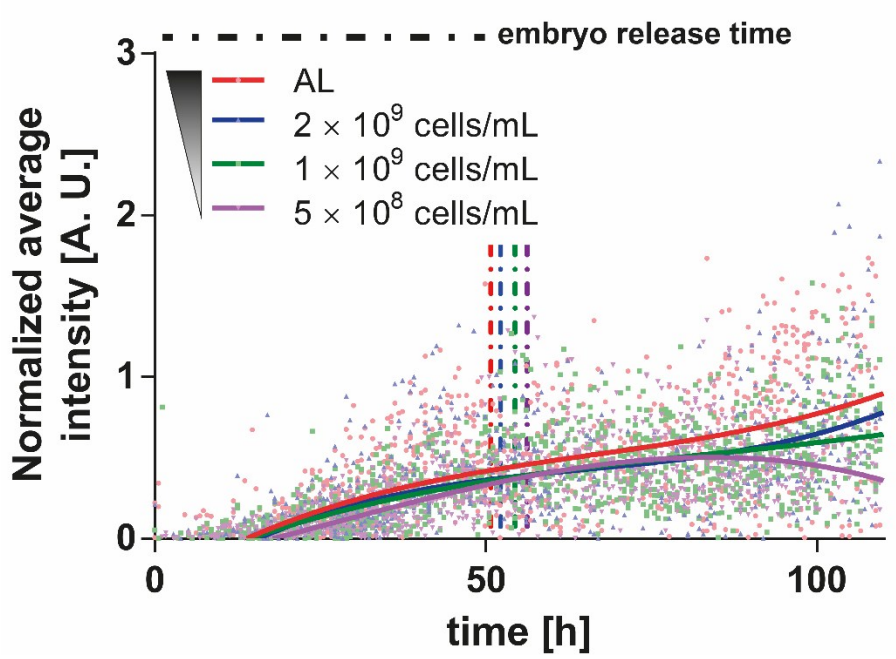

Fig. S10 The normalized average fluorescent intensity expression of *hsp-6::gfp* worms under four different *E. coli* feeding concentrations. A third order polynomial fit is utilized for estimating the normalized average fluorescent intensity in time. R^2 values representing the quality of polynomial fits are calculated to be [0.37, 0.51, 0.59, 0.57] for the feeding conditions [AL, 2×10^9 cells/mL, 1×10^9 cells/mL, 5×10^8 cells/mL], respectively. At the early larval stages, the worms did not have a significant variance in the mitochondrial stress for different amounts of feeding; however, to the later stages of their life cycle, mitochondria were stressed more for a higher feeding concentration than for lower amounts.

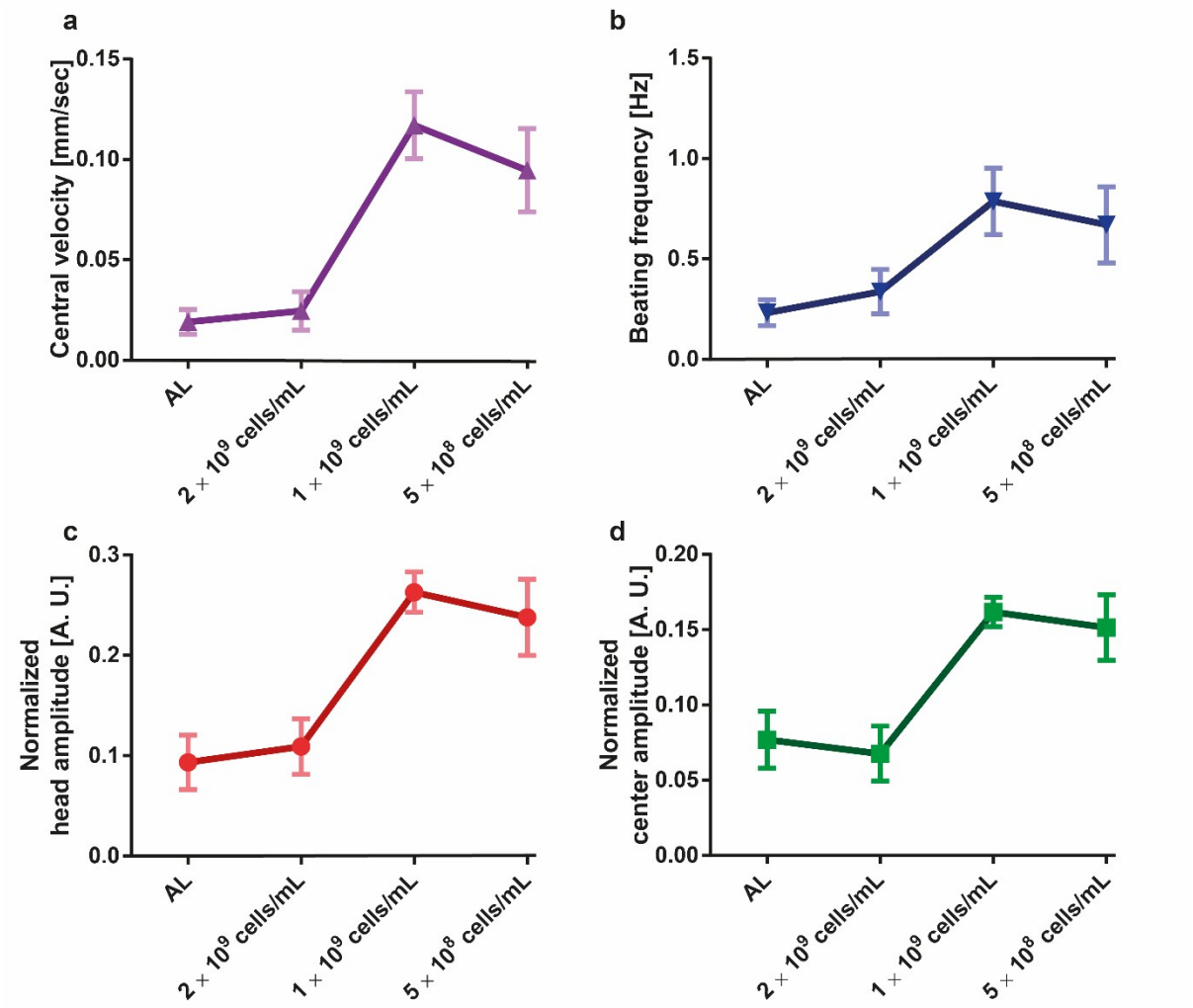

Fig. S11 The dose-dependent motility behavior for four different *E. coli* feeding of *hsp-6::gfp* worms at 57 hours. (a) Central velocity, (b) beating frequency, (c) normalized head beating amplitude and (d) normalized center beating amplitude results compared for four different feeding concentrations are demonstrated. For all the selected motility parameters, there was a gaussian trend. As the food amount decreased, worms tended to increase their motility till a certain point. After that, due to insufficient food provision, worms suffered from caloric restriction.

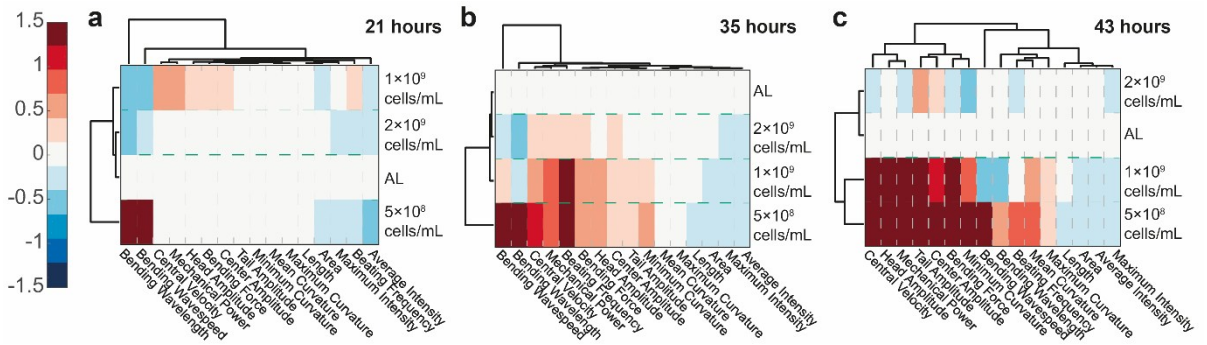

Fig. S12 Clustergram comparison of *hsp-6::gfp* nematodes of motility and development parameters obtained at 21, 35 and 43 hours after the first bacteria injection on the chip, respectively, as obtained for different *E. coli* concentrations. (a) At 21 hours, no significant changes were detected yet, compared to the condition of maximum feeding. Nevertheless, the dendogram related to the lowest *E. coli* concentration started to show distinct features from the other concentrations. (b) The first significant change was detected at 35 hours. The dendogram related to the lowest *E. coli* concentration demonstrated that there was a clear separation from the other feeding concentrations. (c) At 43 hours, the lowest *E. coli* concentration condition and the 1×10^9 cells/mL concentration were coupled together, resulting in a similar behavior of motility parameters and they were separated from the other coupled 2×10^9 cells/mL and AL concentrations. All measurements are based on N=18 to 24 worms.

Supplementary Movies

Movie S1. A real-time video during confinement of L1 worms

Movie S2. A real-time video during confinement of L2 worms

Movie S3. A real-time video during confinement of young adult worms

Movie S4. An illustration of motility tracking of two worms in a growth chamber

Movie S5. Worm distribution via passive hydrodynamics